

## JET BREAK TIME – FLUX DENSITY RELATIONSHIP AND CONSTRAINTS ON PHYSICAL PARAMETERS OF GAMMA-RAY BURST AFTERGLOWS

X. F. WU<sup>1</sup>, Z. G. DAI<sup>1</sup>, AND E. W. LIANG<sup>1,2,3</sup><sup>1</sup>Department of Astronomy, Nanjing University, Nanjing 210093, China; Email:xfwu@nju.edu.cn, dzg@nju.edu.cn, ewliang@nju.edu.cn.<sup>2</sup>Department of Physics, Guangxi University, Nanning 530004, China.<sup>3</sup>National Astronomical Observatories, Yunnan Observatory, Chinese Academy of Sciences, Kunming 650011, China.*Draft version November 14, 2018*

## ABSTRACT

We derive a relation between the flux density  $F_{\nu,j}$  at the light-curve break of a gamma-ray burst (GRB) afterglow and the break time  $t_j$ . The break is due to the transition from the spherical-like to jet-like evolution of the afterglow, when the Lorentz factor of the jet equals the inverse of the initial half-opening angle, i.e.,  $\gamma = 1/\theta_0$ . We show that this relation indeed behaves as  $F_{\nu,j} \propto t_j^{-p}$  among GRBs for the slow-cooling case, where  $p$  is the power-law index of electron distribution. A statistical analysis of the optical jet breaks of nine GRBs gives  $p = 2.10 \pm 0.21$ , which is consistent with the shock acceleration theory. The value of  $p$  derived in this way is different from the observed temporal index  $\alpha_2$  ( $F_{\nu} \propto t^{-\alpha_2}$ ) of the late-time light curve after  $t_j$ , which suffers several uncertainties from the unclear hydrodynamics of the sideways expansion and exhibits a large dispersion. Our results not only confirm that the remnants of GRBs are standard candles, but also provide the first evidence that the physical parameters of relativistic shocks are universal, with the favored values  $\epsilon_e \sim 0.1$  and  $\epsilon_B \sim 10^{-3}$ .

*Subject headings:* gamma rays: bursts—gamma rays: observations—ISM: jets and outflows—methods: statistical

## 1. INTRODUCTION

The gamma-ray burst (GRB) afterglows are attributed to the nonthermal synchrotron/inverse Compton (IC) radiation from the swept-up circumburst electrons shocked by relativistic blast waves (Wijers, Rees & Mészáros 1997; Waxman 1997; Katz & Piran 1997). There are two popular types of circumburst medium, i.e., the interstellar medium (ISM) and the stellar wind (for the latter see Dai & Lu 1998; Mészáros, Rees & Wijers 1998; Chevalier & Li 1999). Nevertheless, the ambient electrons are initially accelerated to a power-law distribution in the same way,  $dN/d\gamma_e \propto \gamma_e^{-p}$  ( $\gamma_m \leq \gamma_e \leq \gamma_{\max}$ ), with the typical index  $p \sim 2.2$ – $2.3$  (Achterberg et al. 2001 and references therein; Lemoine & Pelletier 2003). The minimum Lorentz factor  $\gamma_m$  is proportional to the bulk Lorentz factor  $\gamma$  of the shock and the energy equipartition factor  $\epsilon_e$  of the electrons. Magnetic fields can also be generated by the shock through the relativistic Weibel instability, with the energy equipartition factor  $\epsilon_B$  of  $10^{-5}$  to  $10^{-1}$  (Medvedev & Loeb 1999). The postshock electrons with Lorentz factor  $\gamma_c$  will conveniently lose their total energy in the dynamical timescale because of synchrotron and IC radiation (Sari, Piran & Narayan 1998). The initial distribution of the electrons is thus approximated by a broken power law.

It is now the consensus of most GRB researchers that the GRB fireball is not spherical but indeed conical or jetted. Frail et al. (2001) established the “standard candle” hypothesis of geometrically corrected gamma-ray energy release ( $E_{\gamma} \sim 5 \times 10^{50}$  ergs) of prompt GRBs based on the previous work of Rhoads (1999) and Sari, Piran & Halpern (1999) on the hydrodynamic evolution of a relativistic jet (see also Bloom, Frail & Kulkarni 2003). Panaiteescu & Kumar (2001, 2002) have performed multiwavelength fitting to 10 GRB afterglows and given a comparable mean energy in the jets at the afterglow stage. Statistics of the late-time X-ray luminosity of GRBs further confirms the standard energy outputs in GRB afterglows (Freedman & Wax-

man 2001; Piran et al. 2001; Berger, Kulkarni & Frail 2003). It also requires the small scatter of  $p$  with the mean value  $p \approx 2$  (Berger, Kulkarni & Frail 2003).

In this paper we investigate the energetics of GRB afterglows and the physical parameters related to relativistic shock physics by studying the light curve breaks of GRB optical transients (OTs) in the statistical sense. We derive the analytical relation between the flux density and time at the break in §2. We list the sample and give our statistical results in §3. The findings and implications of our work are discussed in §4.

## 2. SPECTRAL PROPERTIES AT THE JET BREAK TIME

The observed synchrotron spectrum can be determined by the typical frequency  $\nu_m$  corresponding to the electrons with Lorentz factor  $\gamma_m$ , the cooling frequency  $\nu_c$  corresponding to the electrons with Lorentz factor  $\gamma_c$ , and the peak flux density  $F_{\nu,\max}$ . To calculate these quantities, we assume an adiabatic jet with initial half-opening angle  $\theta_0$ . At earlier times, the bulk Lorentz factor  $\gamma$  of the jet is larger than  $\theta_0^{-1}$ , and its radiation shows no difference from that of an isotropic fireball. The light curve steepens achromatically when  $\gamma \leq \theta_0^{-1}$ , because of the deficit of the radiating area for a nonlateral expansion jet or the ultimate change of the hydrodynamics for a lateral-expansion jet. Here we focus on the transitional moment  $t_j$  when  $\gamma = \theta_0^{-1}$  (Sari, Piran & Halpern 1999). The emission properties of an isotropic fireball can be applied to this time, and we derive the flux density  $F_{\nu,j}$  [=  $F_{\nu}(t_j)$ ] as a function of  $t_j$  for both the ISM case and the stellar wind case.

## 2.1. The ISM case

For the ISM case (e.g., Sari et al. 1998), we have

$$t_j = 0.82(1+z)E_{j,51}^{1/3}n^{-1/3}\theta_{0,-1}^2 \text{ days}, \quad (1)$$

$$\nu_{m,j} = 2.7 \times 10^{11} \kappa_m(1+z)^{-1} \epsilon_{e,-1}^2 \epsilon_{B,-3}^{1/2} \zeta_{1/6}^2 n^{1/2} \theta_{0,-1}^{-4} \text{ Hz}, \quad (2)$$

$$\nu_{c,j} = 2.1 \times 10^{16} \kappa_c(1+z)^{-1} \epsilon_{B,-3}^{-3/2} E_{j,51}^{-2/3} n^{-5/6} (1+Y_j)^{-2} \text{ Hz}, \quad (3)$$

$$F_{\nu, \text{max}, j} = 70 \kappa_f (1+z) \epsilon_{B,-3}^{1/2} E_{j,51} \theta_{0,-1}^{-2} n^{1/2} D_{L,28}^{-2} \text{ mJy}, \quad (4)$$

where  $z$  is the redshift,  $D_L$  is the luminosity distance,  $\zeta_{1/6} = 6(p-2)/(p-1)$ ,  $E_j \approx \frac{1}{2} E_{\text{iso}} \theta_0^2$  is the total jet energy, and  $n$  is the density of the ISM in units of  $\text{cm}^{-3}$ . We adopt the convention  $Q = 10^x Q_x$ . We have considered here the accurate expressions for  $\nu_m$ ,  $\nu_c$ , and  $F_{\nu, \text{max}}$ , based on the self-similar solutions of Blandford & McKee (1976) for the spherical blast waves performed by Granot & Sari (2002). The Granot & Sari (2002) corrections to the formulae of Sari, Piran & Narayan (1998) are denoted as  $\kappa_m = 0.73(p-0.67)$ ,  $\kappa_c = (p-0.46)\exp(3.16-1.16p)$ , and  $\kappa_f = 0.09(p+0.14)$ . These factors are nearly constant for  $p$  in the range of 2.0–2.5, and  $\kappa_m = 1.12$ ,  $\kappa_c = 3.22$ , and  $\kappa_f = 0.21$  for  $p = 2.2$ . The Compton parameter  $Y_j = Y(t_j)$  is mainly determined by the ratio  $\epsilon_e/\epsilon_B$  (Panaitescu & Kumar 2000; Sari & Esin 2001). It can be neglected in equation (3) if  $\epsilon_e/\epsilon_B \lesssim 1$ . However, when  $\epsilon_e/\epsilon_B \gg 1$ ,  $\nu_{c,j}$  is rewritten as

$$\begin{aligned} \nu_{c,j} = & 4.5 \times 10^{14} \kappa_c (1+z)^{-1} [1716^{p-2.2} \left(\frac{\kappa_c}{\kappa_m}\right)^{p-2} \epsilon_{e,-1}^{2(1-p)} \epsilon_{B,-3}^{-p/2} \zeta_{1/6}^{2(2-p)} \\ & \times E_{j,51}^{-4/3} \theta_{0,-1}^{4(p-2)} n^{-(3p+4)/6} J^{1/(4-p)} \text{ Hz}, \end{aligned} \quad (5)$$

where the electrons are assumed to be in the IC-dominated slow cooling case at  $t_j$  (Sari & Esin 2001). The transition time from fast cooling to IC-dominated slow-cooling  $t_0^{\text{IC}} = (\epsilon_e/\epsilon_B) t_0 = 5 \times 10^{-4} (\kappa_m/\kappa_c) (1+z) \epsilon_{e,-1}^3 \epsilon_{B,-3} \zeta_{1/6}^2 E_{\text{iso},53} n$  days, measured by the observer, is earlier than typical break time  $t_j \sim 1$  day (see Table 1), while the moment  $t^{\text{IC}}$  when the synchrotron cooling begins to dominate over the IC cooling is typically more than years after the GRB trigger (Sari & Esin 2001).

The flux density at the jet break time in the slow-cooling spectrum case ( $\nu_m < \nu < \nu_c$ ) is

$$\begin{aligned} F_{\nu,j} = & 70 t_{j,\text{day}}^{-p} \times 73.7^{2.2-p} \kappa_f \kappa_m^{(p-1)/2} \epsilon_{e,-1}^{p-1} \epsilon_{B,-3}^{(p+1)/4} \zeta_{1/6}^{p-1} n^{(3-p)/12} \\ & \times E_{j,50.5}^{(p+3)/3} D_{L,28}^{-2} (1+z)^{(p+3)/2} \left(\frac{\nu}{\nu_R}\right)^{-(p-1)/2} \mu\text{Jy}, \end{aligned} \quad (6)$$

where  $\nu_R = 4.55 \times 10^{14}$  Hz is the  $R$ -band frequency taken as the observed frequency. Equation (6) provides a relationship between the flux density  $F_{\nu,j}$  and the jet break time  $t_j$ . In the following this relationship is called the jet break relation. On the other hand, a similar relation in the fast-cooling case ( $\nu_c < \nu$ ) follows

$$\begin{aligned} F_{\nu,j} = & 700 t_{j,\text{day}}^{-p} \times 73.7^{2.2-p} \kappa_f \kappa_m^{(p-1)/2} \kappa_c^{1/2} D_{L,28}^{-2} \epsilon_{e,-1}^{p-1} \epsilon_{B,-3}^{(p-2)/4} \zeta_{1/6}^{p-1} \\ & \times E_{j,50.5}^{(p+2)/3} n^{-(p+2)/12} (1+z)^{(p+2)/2} (1+Y_j)^{-1} \left(\frac{\nu}{\nu_R}\right)^{-p/2} \mu\text{Jy}, \end{aligned} \quad (7)$$

which can be rewritten as

$$\begin{aligned} F_{\nu,j} = & 114 t_{j,\text{day}}^{-p+(p-2)/(4-p)} \times 73.7^{2.2-p} \kappa_f \kappa_m^{p/2} D_{L,28}^{-2} \left(\frac{\nu}{\nu_R}\right)^{-p/2} \\ & \times [121^{p-2.2} \left(\frac{\kappa_c}{\kappa_m}\right)^{2p-p^2-3} \epsilon_{e,-1}^{(4+2p-p^2)/4} \epsilon_{B,-3}^{4p-p^2-2} E_{j,50.5}^{(12-p^2)/3} \\ & \times n^{p(p-6)/12} (1+z)^{(12-p^2)/2}]^{1/(4-p)} \mu\text{Jy}, \end{aligned} \quad (8)$$

in the limit of  $\epsilon_e/\epsilon_B \gg 1$ , where we do not include the contribution of the synchrotron-self-Compton (SSC) scattering to the flux density, since the SSC component always appears above the X-ray band for typical physical parameters and the light curve breaks are mostly observed in optical band.

## 2.2. The stellar wind case

For the stellar wind case (e.g., Chevalier & Li 2000), we have

$$t_j = 1.25(1+z) E_{j,51} A_*^{-1} \theta_{0,-1}^2 \text{ days}, \quad (9)$$

$$\nu_{m,j} = 2.9 \times 10^{11} \kappa_m (1+z)^{-1} \epsilon_{e,-1}^2 \epsilon_{B,-3}^{1/2} \zeta_{1/6}^2 E_{j,51}^{-1} A_*^{3/2} \theta_{0,-1}^{-4} \text{ Hz}, \quad (10)$$

$$\nu_{c,j} = 2.8 \times 10^{16} \kappa_c (1+z)^{-1} \epsilon_{B,-3}^{-3/2} E_{j,51} A_*^{-5/2} (1+Y_j)^{-2} \text{ Hz}, \quad (11)$$

$$F_{\nu, \text{max}, j} = 7.45 \kappa_f (1+z) \epsilon_{B,-3}^{1/2} A_*^{3/2} \theta_{0,-1}^{-2} D_{L,28}^{-2} \text{ mJy}, \quad (12)$$

where  $A_*$  is the wind parameter (Chevalier & Li 1999). The correction factors derived from Granot & Sari (2002) are  $\kappa_m = 0.4(p-0.69)$ ,  $\kappa_c = (3.45-p)\exp(0.45p-1.4)$ , and  $\kappa_f = 1.31(p+0.12)$ . For  $p = 2.2$ ,  $\kappa_m = 0.60$ ,  $\kappa_c = 0.83$ , and  $\kappa_f = 3.04$ . When  $\epsilon_e/\epsilon_B \gg 1$ , the transition time from fast cooling to IC-dominated slow cooling in the wind case is  $t_0^{\text{IC}} = (\epsilon_e/\epsilon_B)^{1/2} t_0 = 4 \times 10^{-2} (\kappa_m/\kappa_c)^{1/2} (1+z) \epsilon_{e,-1}^{3/2} \epsilon_{B,-3}^{1/2} \zeta_{1/6} A_*$  days, which is earlier than  $t_j \sim 1$  day. In this case  $\nu_{c,j}$  is rewritten as

$$\begin{aligned} \nu_{c,j} = & 6.0 \times 10^{14} \kappa_c (1+z)^{-1} [2151^{p-2.2} \left(\frac{\kappa_c}{\kappa_m}\right)^{2(p-2)} \epsilon_{e,-1}^{2(1-p)} \epsilon_{B,-3}^{-p/2} \zeta_{1/6}^{2(2-p)} \\ & \times E_{j,51}^p \theta_{0,-1}^{4(p-2)} A_*^{-(3p+4)/2}]^{1/(4-p)} \text{ Hz}. \end{aligned} \quad (13)$$

The flux density at the jet break time in the slow-cooling case ( $\nu_m < \nu < \nu_c$ ) is

$$\begin{aligned} F_{\nu,j} = & 23 t_{j,\text{day}}^{-p} \times 57.3^{2.2-p} \kappa_f \kappa_m^{(p-1)/2} \epsilon_{e,-1}^{p-1} \epsilon_{B,-3}^{(p+1)/4} \zeta_{1/6}^{p-1} A_*^{(3-p)/4} \\ & \times E_{j,50.5}^{(p+1)/2} D_{L,28}^{-2} (1+z)^{(p+3)/2} \left(\frac{\nu}{\nu_R}\right)^{-(p-1)/2} \mu\text{Jy}, \end{aligned} \quad (14)$$

while the density flux at  $\nu_c < \nu$  becomes

$$\begin{aligned} F_{\nu,j} = & 100 t_{j,\text{day}}^{-p} \times 57.3^{2.2-p} \kappa_f \kappa_m^{(p-1)/2} \kappa_c^{1/2} D_{L,28}^{-2} \epsilon_{e,-1}^{p-1} \epsilon_{B,-3}^{(p-2)/4} \zeta_{1/6}^{p-1} \\ & \times E_{j,50.5}^{(p+2)/2} A_*^{-(p+2)/4} (1+z)^{(p+2)/2} (1+Y_j)^{-1} \left(\frac{\nu}{\nu_R}\right)^{-p/2} \mu\text{Jy} \end{aligned} \quad (15)$$

which can be further deduced in the case of  $\epsilon_e/\epsilon_B \gg 1$ ,

$$\begin{aligned} F_{\nu,j} = & 14.5 t_{j,\text{day}}^{-p+(p-2)/(4-p)} \times 57.3^{2.2-p} \kappa_f \kappa_m^{p/2} D_{L,28}^{-2} \left(\frac{\nu}{\nu_R}\right)^{-p/2} \\ & \times E_{j,50.5}^{(p+2)/2} [36.2^{p-2.2} \left(\frac{\kappa_c}{\kappa_m}\right)^{p/2} \epsilon_{e,-1}^{2p-p^2-3} \epsilon_{B,-3}^{(4+2p-p^2)/4} \zeta_{1/6}^{4p-p^2-6} \\ & \times A_*^{p(p-6)/4} (1+z)^{(12-p^2)/2}]^{1/(4-p)} \mu\text{Jy}. \end{aligned} \quad (16)$$

We can see that in the slow-cooling case, the jet break relation behaves as  $F_{\nu,j} \propto t_j^{-p}$  among GRB afterglows, as long as the physical parameters  $E_j$ ,  $\epsilon_e$ , and  $\epsilon_B$  are clustered. This relation is assured in both the ISM and the stellar wind case, and is insensitive to the medium density in each case. It provides a tool for probing the energetics of GRB afterglows and the shock physics of relativistic blast waves. The jet break relation of the fast-cooling case is affected by the Compton parameter  $Y_j$ . If  $Y_j < 1$ , the jet break relation becomes  $F_{\nu,j} \propto t_j^{-p}$  and is insensitive to  $\epsilon_B$  while moderately sensitive to the ambient medium density. If  $Y_j > 1$ , the relation changes to  $F_{\nu,j} \propto t_j^{-p+(p-2)/(4-p)}$ , in which the index  $p-(p-2)/(p-4)$  is in the range of 2.0–2.17 for  $p \sim 2.0$ –3.0.

### 3. STATISTICAL RESULTS

#### 3.1. The sample

In Table 1 we give an updated optical  $R$ -band sample of 14 GRB light curve breaks. Our sample is slightly different from the Bloom et al. (2003; hereafter BFK03) sample. In the BFK03 sample of 17 GRBs with known  $t_j$ , they included six jet breaks that were determined from observations outside the optical bands, e.g., GRBs 970508, 980703, and 000418 at the radio band; GRB 990705 at  $H$  band; GRB 010921 at the joint  $I$  and F702 W bands; and GRB 970828 at the X-ray band. Recently, two new  $R$ -band jet breaks of GRBs 030226 and 030329 have been observed. Greiner et al. (2003a) concluded that a jet break existed in the  $R$ -band light curve of the GRB 011121 afterglow before 10 days. We also add this GRB in Table 1. Since the error of  $t_j$  of GRB 011121 is large, it will not significantly change our statistical results. There are two peculiar OTs in our sample. GRB 000301C showed a prebreak bump in the optical afterglow that has been explained as being caused by the central engine activity, by the external density jump, or by the microlensing event (Bhargavi & Cowsik 2000; Dai & Lu 2001, 2002; Garnavich, Loeb & Stanek 2000). GRB 021004 also exhibited complicated fluctuations in the early afterglow before the temporal break (Fox et al. 2003).

In Table 2 we give a sample of five fast-fading GRB optical afterglows. Fast-fading afterglows are believed to be already in the jet-like stages before they are definitely observed. The upper limit of  $t_j$  is the time when the first positive optical detection was made. We exclude GRB 980329 in the BFK03 sample because the temporal index is relatively too shallow to be identified as a fast-fading GRB ( $\alpha = 1.28 \pm 0.19$ ; Reichart et al. 1999). The optical afterglow of GRB 990705 may be a fast-fading one, but there is no reliable  $R$ -band data for this GRB.

#### 3.2. Results

From Table 1 we can see that the optical spectral index  $\beta_{\text{opt}}$  around  $t_j$  is less than 0.8 for most GRB OTs. This can be interpreted as the optical frequency located at the slow-cooling segment ( $\nu_m < \nu < \nu_c$ ) of the spectrum, since the observed index is consistent with the theoretical one,  $\beta = (p-1)/2 \sim 0.6-0.75$  for  $p \sim 2.2-2.5$ . There are two outliers, GRB 000926 and 020813, which have relatively steep spectra at  $t_j$  and can be regarded to be in the fast-cooling case in which the typical spectral index  $\beta = p/2 \sim 1.1$ . We thus adopt the jet break relation of the slow-cooling case for the statistical purpose in this work.

To decouple the effects of the redshift and the luminosity distance from other parameters, we rewrite equations (6) and (14), and the general jet break relation in the slow-cooling case is

$$\mathcal{L}_J = a - b\tau_j, \quad (17)$$

where  $\mathcal{L}_J \equiv \log[F_{\nu,j}D_{L,28}^2(1+z)^{-3/2}/\mu\text{Jy}]$  and  $\tau_j \equiv \log[t_j(1+z)^{-1/2}/\text{days}]$  are the equivalent luminosity density and jet break time in logarithms, which can be determined directly by observations. The coefficient  $a$  is a combination of the physical parameters of the central engine and the shock physics and is insensitive to the external medium density. However,  $b \equiv p$  is only determined by the index of the distribution of the electrons. We adopt the cosmology with  $\Omega_m = 0.27$ ,  $\Omega_\Lambda = 0.73$ , and  $H_0 = 71 \text{ km s}^{-1} \text{ Mpc}^{-1}$ .

<sup>1</sup>The linear fit method is from Press et al. 1992.

<sup>2</sup>The relative error is  $< 2\%$  for  $z < 2$ ,  $< 14\%$  for  $z \sim 2-100$ , and  $< 5\%$  for  $z > 200$ . At very small and large  $z$ , the relative error approaches to zero. However, we use the exact integral formula of  $D_L$  in our calculations.

Figure 1 shows the  $\mathcal{L}_J - \tau_j$  plot for 11 GRBs with known redshifts. Excluding GRBs 000926 and 020813 as explained above, we have made the best linear fit to the remaining nine GRB OT breaks using equation (17).<sup>1</sup> The derived values and standard errors are  $a = 1.37 \pm 0.05$ ,  $b = 2.10 \pm 0.21$ , the corresponding  $\chi^2 = 9.97$  for 7 degrees of freedom (dof), and the possibility  $Q(> \chi^2) = 0.19$ . If we do not include GRB 011121, the result gives the same  $a$  and  $b$ , while  $\chi^2 = 9.67$  for 6 dof and  $Q(> \chi^2) = 0.14$ . This can be explained by the large error bar of this GRB, as shown in Figure 1. The mean value of  $b$  is consistent with the theoretical value of  $p$  (Achterberg et al. 2001). The large scatter of  $b$  is caused by the limitation of the small sample. If we adopt  $a = 1.37 \pm 0.15$  ( $3\sigma$ ) and  $b = 2.2$ , the jet break relation constrains the physical parameters as

$$\begin{aligned} \epsilon_{e,-1}^{1.2} \epsilon_{B,-3}^{0.8} n^{0.07} E_{j,50.5}^{1.73} &\sim 1.1-2.1 \text{ (ISM),} \\ \epsilon_{e,-1}^{1.2} \epsilon_{B,-3}^{0.8} A_{*,-1}^{0.2} E_{j,50.5}^{1.6} &\sim 0.51-1.0 \text{ (wind),} \end{aligned} \quad (18)$$

which implies the *universal* energy reservoir and relativistic shock physics. The constraints for the ISM case and the wind case are nearly the same, as long as the typical wind parameter is relatively small,  $A_* = 0.1$  (Wu et al. 2003; Dai & Wu 2003; Chevalier, Li & Fransson 2004). The determination of the intrinsic mean values of these parameters is needed to combine equation (18) with other methods, e.g., the multiwavelength fits to the overall afterglow light curves. Panaiteescu & Kumar (2001, 2002) have performed these fits and given the mean values of  $E_j \sim 5 \times 10^{50}$  ergs,  $\epsilon_e \sim 0.3$ , and  $\epsilon_B \sim 4 \times 10^{-3}$ , which are marginally consistent with the constraints of equation (18). We note that Panaiteescu & Kumar (2001, 2002) have assumed the distribution of initially shocked electrons to be a broken power law. They have also given a large range of  $\epsilon_B$ , from  $10^{-5}$  to 0.1. Although the lower and upper limits of  $\epsilon_B$  are expected when the relativistic two-stream instability of the electrons and protons saturates separately (Medvedev & Loeb 1999), the question is why the same relativistic shock physics leads to very different  $\epsilon_B$  values among GRB afterglows. In this work, we prefer the mean values of physical parameters as  $E_j \sim 3 \times 10^{50}$  ergs,  $\epsilon_e \sim 0.1$ , and  $\epsilon_B \sim 10^{-3}$ .

In Figure 2 we calculate the  $\mathcal{L}_J - \tau_j$  plot for GRB 980519 at different redshift. The line of GRB 980519 can be understood as the luminosity distance  $D_L$  as a function of  $z$ , which can be approximated by<sup>2</sup>

$$D_L(z) = \frac{c}{H_0} \frac{1+z}{1+0.29z} z, \quad (19)$$

for  $\Omega_m = 0.27$  and  $\Omega_\Lambda = 0.73$ , where  $c$  is the speed of light. The line begins vertically when  $z \ll 1$  and approaches a diagonal with a slope of  $-1$  at  $z \gg 1$  in the  $\mathcal{L}_J - \tau_j$  plot. If GRB 980519 obeys the same jet break relation of equation (17), a lower limit of its redshift,  $z \gtrsim 1.65$ , is indicated in Figure 2. This lower limit is consistent with the nondetection of a supernova signature expected to accompany GRB 980519 at late times, which implies  $z \gtrsim 1.5$  (Jaunsen et al. 2001). However, the redshift determined by the jet break relation has, in general, two values. The specific jet break data of GRB 980519 and the large scatter of  $t_j$  prevent the unambiguous determination of its redshift.

Figure 3 shows the break data of two peculiar GRBs, GRB 000301C and 021004, and five fast-fading GRBs, together with

11 typical GRB breaks with known redshifts. Fluctuations or bumps in the optical light curve before  $t_j$  will strongly affect the observational determination of  $t_j$ . However, it is impossible to attribute GRB 000301C and 021004 to the universal class obeying the same jet break relation, because of the uncertainty of their  $t_j$  and  $F_{\nu,j}$ . A rough estimate of the physical parameters assuming the same  $b = 2.1$  for these two GRBs will give  $a \sim 2.75$ , twice the universal value. Since  $a$  is insensitive to the external number density, and since it is unreasonable to assume the shock physics will change much in short timescales, we draw an exclusive conclusion that the jet is re-energized by a factor of 6.3 (7.3) for ISM (wind) case, because of the delayed energy injection from the central engine. Bloom, Frail & Kulkarni (2003) proposed that fast-fading GRBs belong to the low-energy subclass with respect to the gamma-ray energy release. However, the case becomes more complicated in view of the residual energy in the afterglow epoch, as shown in Figure 3. The fast-fading GRB 000131 seems to obey the jet break relation, because the line extrapolating its first detected data to the earlier time  $t_j$  is nearly parallel to the solid line, since  $\alpha \sim b$ . GRB 000911 also seems to belong to the universal class, if the first detection time is close to the true  $t_j$ . GRB 980326 is identified as a subenergetic GRB afterglow. The spectral indices of GRBs 991208 and 001007 indicate that they belong to the fast-cooling case, although the indices are not corrected for the host galaxy extinction, which may make them possibly belong to the slow-cooling case. For comparison, they are plotted in Figure 3. The redshift of GRB 001007 is estimated at  $z \sim 0.18$  by assuming that it follows the slow-cooling jet break relation. However, a reliable redshift can be only estimated when a large sample of fast-cooling jet break data is achieved.

#### 4. CONCLUSIONS AND DISCUSSION

In this paper, we have derived the jet break relation of GRB optical light curves,  $F_{\nu,j} \propto t_j^{-p}$ , and given the statistical results of this relation based on the available sample. Now we summarize our findings and discuss their implications.

First, the electron distribution index  $p = 2.10 \pm 0.21$  is achieved in the statistical sense. Conventionally, the late temporal index  $\alpha_2$  or  $\alpha$  of fast-fading GRBs is believed to be the same as  $p$ . However, there are two caveats on this assumption. (1) Most importantly, the ambiguity of the understanding of the sideways expansion of the jet leads to a great uncertainty of the value of  $\alpha_2$ . For a non-lateral spreading jet,  $\alpha_2$  is larger than  $\alpha_1$  by 3/4 (1/2) for ISM (wind) case, because of the deficit of the visual edge caused by the relativistic beaming effect (Mészáros & Rees 1999). GRBs 990123, 010222, 020813, 021004, and the fast-fading GRB 000911 are candidates for nonlateral expansion jets. It should be pointed out that an explanation with flat electron spectra of  $1 < p < 2$  fails to account for these bursts, since in this case  $\alpha_2 = (p+6)/4 (> 1.75)$  is larger than the observed value (Dai & Cheng 2001). (2) Even

though detailed calculation of sideways expansion evolution results in the light curve of  $\alpha_2 \sim p$ , there is a tendency for larger  $\theta_0$  to cause relatively flatter  $\alpha_2$  (Huang, Dai & Lu 2000; Wu et al. 2004). There is also an indication that  $\alpha_2$  is larger (steeper) than  $p$  in the two-dimensional simulation (Granot et al. 2001). In this case, the jet experiences a lateral expansion stage, while the emission is mostly arising from the part of the initial half-opening angle. The temporal index of the steepest light curve in this case is estimated to be  $\alpha_2 \sim p+1$ . However, the jet break relation is determined at  $t_j$ , and the only assumption is  $\gamma(t_j) = \theta_0^{-1}$  (Frail et al. 2001). The value of  $p = b$  derived from this relation avoids the above uncertainties and can be used as a better and independent way to constrain the relativistic shock acceleration physics.

Second, the jet break relation further supports the “standard candle” hypothesis of the afterglows (Panaitescu & Kumar 2001, 2002; Freedman & Waxman 2001; Piran et al. 2001; Bloom, Frail & Kulkarni 2003; Berger, Kulkarni & Frail 2003). Furthermore, it also constrains the shock physics to be universal among nine GRBs in the slow-cooling case (see equation 18). Since the jet break relation is almost immune from the effect of external density, it can probe the energy reservoir and shock physics of GRBs at high redshifts, where the density of the ISM or the stellar wind may significantly follow the cosmological evolution (Ciardi & Loeb 2000). There is another capability of this relation to distinguish between some peculiar GRBs, e.g., the GRBs with delayed energy injections before  $t_j$ .

Third, as a by-product, we can estimate the redshift of some jet break GRBs or fast-fading GRBs by using of the jet break relation, assuming they follow the standard energy and same shock physics.

The jet break relation itself can not distinguish between the structures of GRBs jets (Mészáros, Rees & Wijers 1998; Dai & Gou 2001; Rossi, Lazzati & Rees 2002; Zhang, & Mészáros 2002). However, the empirical formula that is used to fit the light curves gives the required jet break data, e.g.,  $F_{\nu,j}$ ,  $t_j$ , and the break sharpness  $s$  (Beuermann et al. 1999; Rhoads & Fruchter 2001). The sharpness  $s$  has the potential to probe the jet structure, because it behaves in a different way as a function of  $\theta_0$  (therefore  $t_j$ ) in a homogeneous jet and in a structured jet.

The  $F_{\nu,j} - t_j$  relation presents a way to constrain the value of  $p$  and other physical parameters of GRB afterglows. A more robust result should be based on a larger sample of GRBs with measured jet breaks in their afterglow light curves, which is expected in the upcoming *Swift* era.

We thank the referee very much for his/her valuable suggestions and comments. This work was supported by the National Natural Science Foundation of China (grants 10233010 and 10221001), the Ministry of Science and Technology of China (NKBRSF G19990754), the Natural Science Foundation of Yunnan (2001A0025Q), and the Research Foundation of Guangxi University.

#### REFERENCES

- Achterberg, A., Gallant, Y. A., Kirk, J. G., & Guthmann, A. W. 2001, MNRAS, 328, 393
- Anderson, M. I., et al. 2000, A&A, 364, L54
- Barth, A. J., et al. 2003, ApJ, 584, L47
- Berger, E., Soderberg, A. M., Frail, D. A., & Kulkarni, S. R. 2003, ApJ, 587, L5
- Berger, E., Kulkarni, S. R., & Frail, D. A. 2003, ApJ, 590, 379
- Beuermann, K., et al. 1999, A&A, 352, L26
- Bhargavi, S. G., & Cowsik, R. 2000, ApJ, 545, L77
- Blandford, R. D., & McKee, C. F. 1976, Phys. Fluids, 19, 1130
- Bloom, J. S., et al. 1999, Nature, 401, 453

Bloom, J. S., Frail, D. A., & Kulkarni, S. R. 2003, *ApJ*, 594, 674

Castro, S. M., et al. 2000, *GCN CirC*, 851

Castro Cerón, J. M., et al. 2002, *A&A*, 393, 445

Castro-Tirado, A. J., et al. 2001, *A&A*, 370, 398

Chevalier, R. A., & Li, Z. Y. 1999, *ApJ*, 520, L29

Chevalier, R. A., & Li, Z. Y. 2000, *ApJ*, 536, 195

Chevalier, R. A., Li, Z. Y., & Fransson, C. 2004, *ApJ*, 606, 369

Ciardi, B., & Loeb, A. 2000, *ApJ*, 540, 687

Covino, S., et al. 2003, *A&A*, 404, L5

Dai, Z. G., & Lu, T. 1998, *MNRAS*, 298, 87

Dai, Z. G., & Cheng, K. S. 2001, *ApJ*, 558, L109

Dai, Z. G., & Lu, T. 2001, *A&A*, 367, 501

Dai, Z. G., & Gou, L. J. 2001, *ApJ*, 552, 72

Dai, Z. G., & Lu, T. 2002, *ApJ*, 565, L87

Dai, Z. G., & Wu, X. F. 2003, *ApJ*, 591, L21

Fox, D. W., et al. 2003, *Nature*, 422, 284

Frail, D. A., et al. 2001, *ApJ*, 562, L55

Freedman, D. L., & Waxman, E. 2001, *ApJ*, 547, 922

Fruchter, A., Vreeswijk, P., Rhoads, J., & Burud, I. 2001, *GCN CirC*, 1200

Galama, T. J., et al. 2003, *ApJ*, 587, 135

Garnavich, P. M., Jha, S., Pahre, M. A., Stanek, K. Z., Kirshner, R. P., Garcia, M. R., Szentgyorgyi, A. H., & Tonry, J. L. 2000, *ApJ*, 543, 61

Garnavich, P. M., Loeb, A., & Stanek, K. Z. 2000, *ApJ*, 544, 11

Garnavich, P. M., et al. 2003, *ApJ*, 582, 924

Granot, J., Miller, M., Piran, T., Suen, W. M., & Hughes, P. A. 2001, in *Gamma-Ray Bursts in the Afterglow Era*, ed. E. Costa, F. Frontera, & J. Hjorth (Berlin: Springer), 312

Granot, J., & Sari, R. 2002, *ApJ*, 568, 820

Greiner, J., Guenther, E., Klose, S., & Schwarz, R. 2003a, *GCN CirC*, 1886, <http://gcn.gsfc.nasa.gov/gcn/gcn3/1886.gcn3>

Greiner, J., et al. 2003b, *ApJ*, 599, 1223

Greiner, J., et al. 2003c, *GCN CirC*, 2020, <http://gcn.gsfc.nasa.gov/gcn/gcn3/2020.gcn3>

Halpern, J. P., et al. 2000, *ApJ*, 543, 697

Holland, S. T., Björnsson, G., Hjorth, J., & Thomsen, B. 2000, *A&A*, 364, 467

Holland, S. T., et al. 2002, *AJ*, 124, 639

Holland, S. T., et al. 2003, *AJ*, 125, 2291

Huang, Y. F., Dai, Z. G., & Lu, T. 2000, *MNRAS*, 316, 943

Jakobsson, P., et al. 2003, *A&A*, 408, 941

Jaunsen, A. O., et al. 2001, *ApJ*, 546, 127

Jensen, B. L., et al. 2001, *A&A*, 370, 909

Jensen, B. L., et al. 1999, *GCN CirC*, 454

Jha, S., et al. 2001, *ApJ*, 554, L155

Katz, J. I., & Piran, T. 1997, *ApJ*, 490, 772

Kulkarni, S. R., et al. 1999, *Nature*, 398, 389

Lazzati, D., et al. 2001, *A&A*, 378, 996

Lemoine, M., & Pelletier, G. 2003, *ApJ*, 589, L73

Matheson, T., et al. 2003, *ApJ*, 599, 394

Medvedev, M. V., & Loeb, A. 1999, *ApJ*, 526, 697

Mészáros, P., Rees, M., & Wijers, R. A. M. J. 1998, *ApJ*, 499, 301

Mészáros, P., & Rees, M. J. 1999, *MNRAS*, 306, L39

Mirabal, N., Paerels, F., & Halpern, J. P. 2003, *ApJ*, 587, 128

Møller, P., et al. 2002, *A&A*, 396, L21

Panaiteescu, A., & Kumar, P. 2000, *ApJ*, 543, 66

Panaiteescu, A., & Kumar, P. 2001, *ApJ*, 560, L49

Panaiteescu, A., & Kumar, P. 2002, *ApJ*, 571, 779

Pandey, S. B., Sagar, R., Anupama, G. C., Bhattacharya, D., Sahu, D. K., Castro-Tirado, A. J., & Bremer, M. 2004, *A&A*, 417, 919

Piran, T., Kumar, P., Panaiteescu, A., & Piro, L. 2001, *ApJ*, 560, L167

Press, W. H., Teukolsky, S. A., Vetterling, W. T., & Flannery, B. P. 1992, *Numerical Recipes in C* (Cambridge University Press)

Price, P. A., et al. 2002, *ApJ*, 573, 85

Price, P. A., et al. 2003, *ApJ*, 589, 838

Reichart, D. E., et al. 1999, *ApJ*, 517, 692

Rhoads, J. E. 1999, *ApJ*, 525, 737

Rhoads, J. E., & Fruchter, A. S. 2001, *ApJ*, 546, 117

Rossi, E., Lazzati, D., & Rees, M. J. 2002, *MNRAS*, 332, 945

Sagar, R., Pandey, S. B., Mohan, V., Bhattacharya, D., & Castro-Tirado, A. J. 2001, *BASI*, 29, 1

Sari, R., Piran, T., & Narayan, R. 1998, *ApJ*, 497, L17

Sari, R., Piran, T., & Halpern, J. P. 1999, *ApJ*, 519, L17

Sari, R., & Esin, A. A. 2001, *ApJ*, 548, 787

Sato, R., Kawai, N., Suzuki, M., Yatsu, Y., Kataoka, J., Takagi, R., Yanagisawa, K., & Yamaoka, H. 2003, *ApJ*, 599, L9

Stanek, K. Z., Garnavich, P. M., Kaluzny, J., Pych, W., & Thompson, I. 1999, *ApJ*, 522, L39

Urata, Y., et al. 2003, *ApJ*, 595, L21

Vreeswijk, P. M., Fruchter, A., Ferguson, H., & Kouveliotou, C. 1999, GCN CirC. 751  
Vreeswijk, P. M., et al. 2001, ApJ, 546, 672  
Waxman, E. 1997, ApJ, 485, L5  
Wijers, R. A. M. J., Rees, M. J., & Mészáros, P. 1997, MNRAS, 288, L51  
Wu, X. F., Dai, Z. G., Huang, Y. F., & Lu, T. 2003, MNRAS, 342, 1131  
Wu, X. F., Dai, Z. G., Huang, Y. F., & Ma, H. T. 2004, ChJAA, in press (astro-ph/0311358)  
Zhang, B., & Mészáros, P. 2002, ApJ, 571, 876

TABLE 1  
*R*-BAND JET BREAK DATA

GRB	$z$	$\alpha_1$	$\alpha_2$	$t_j$ (day)	$F_{\nu,j}$ ( $\mu$ Jy)	$\beta_{\text{opt}}(t_{\text{day}})^c$	Reference
980519	...	$1.73 \pm 0.04$	$2.22 \pm 0.04$	$0.55 \pm 0.20$	$31.6 \pm 3.16^b$	$0.81 \pm 0.01(0.45)$	1
990123	1.6004	$1.17 \pm 0.30$	$1.57 \pm 0.11$	$1.70 \pm 0.22$	$10.74 \pm 3.01$	$0.75 \pm 0.07(< 2.8)$	2,3
990510	1.6187	$0.46 \pm 0.20$	$1.85 \pm 0.26$	$0.70 \pm 0.35$	$114.54 \pm 63.24$	$0.61 \pm 0.12(0.9)$	4,3,5
991216	1.02	1.0	1.8	$1.20 \pm 0.40$	$30 \pm 3^b$	$0.58 \pm 0.08(1.65)$	6,7,8
000301C <sup>a</sup>	2.0404	$0.72 \pm 0.06$	$2.29 \pm 0.17$	$4.39 \pm 0.26$	$16.23 \pm 1.13$	$\sim 0.6(4.26)$	9,10
000926	2.0369	$1.45 \pm 0.06$	$2.57 \pm 0.10$	$1.74 \pm 0.11$	$9.38_{-1.21}^{+1.39}$	$0.94 \pm 0.02(2.26)$	11,12
010222	1.4768	$\sim 0.8$	$1.57 \pm 0.04$	$0.93_{-0.06}^{+0.15}$	$30.45_{-2.5}^{+5.1}$	$0.75(< 2.96)$	13,14
011121	0.362	$1.62 \pm 0.39$	$2.44 \pm 0.34$	$1.20 \pm 0.75$	$22.0 \pm 2.2^b$	$0.62 \pm 0.05(2.5)$	15,16
011211	2.140	$0.95 \pm 0.02$	$2.11 \pm 0.07$	$1.56 \pm 0.02$	$6.31 \pm 0.63^b$	$0.61 \pm 0.15(< 1.52)$	17,18,19
020405	0.6899	$\sim 1.4$	$\sim 1.95$	$0.95 \pm 0.04$	$50 \pm 5^b$	$0.74(1.7)$	20,21,22
020813	1.255	$0.76 \pm 0.05$	$1.46 \pm 0.04$	$0.57 \pm 0.05$	$38.0 \pm 3.8^b$	$0.93 \pm 0.16(0.43)$	23,24,25
021004 <sup>a</sup>	2.3351	$0.85 \pm 0.01$	$1.43 \pm 0.03$	$4.74_{-0.80}^{+0.14}$	$14.675_{-0.445}^{+3.209}$	$0.39 \pm 0.12(5.57)$	26,27
030326	1.986	$0.77 \pm 0.04$	$1.99 \pm 0.06$	$0.69 \pm 0.04$	$29.65_{-1.59}^{+1.68}$	$\sim 0.55(0.62)$	28,29
030329	0.1685	$1.18 \pm 0.01$	$1.81 \pm 0.04$	$0.54 \pm 0.05^b$	$3020 \pm 302^b$	$0.71(0.65)$	30,31,32

NOTE.—Col.(1) GRB name; col.(2) redshift; col.(3) temporal decay index ( $F_{\nu} \propto t^{-\alpha_1}$ ) before  $t_j$ ; col.(4) temporal decay index ( $F_{\nu} \propto t^{-\alpha_2}$ ) after  $t_j$ ; col.(5) observed jet break time; col.(6) flux density at  $t_j$ ; col.(7) optical spectrum  $F_{\nu} \propto \nu^{-\beta_{\text{opt}}}$  at time  $t$  in days since the GRB trigger; and col.(8) references for the redshift and *R*-band afterglow. <sup>a</sup>These two peculiar GRB OTs showed fluctuations in their early light curves. <sup>b</sup>We estimate 10% uncertainties for these quantities which were not directly given in the literature. <sup>c</sup>The value of  $\beta_{\text{opt}}$  is sensitive to the assumed host galaxy extinction correction.

REFERENCES.— (1) Jaunsen et al. 2001; (2) Kulkarni et al. 1999; (3) Holland et al. 2000; (4) Vreeswijk et al. 2001; (5) Stanek et al. 1999; (6) Vreeswijk et al. 1999; (7) Halpern et al. 2000; (8) Garnavich et al. 2000; (9) Jensen et al. 2001; (10) Rhoads & Fruchter 2001; (11) Castro et al. 2000; (12) Sagar et al. 2001; (13) Jha et al. 2001; (14) Galama et al. 2003; (15) Garnavich et al. 2003; (16) Greiner et al. 2003b; (17) Fruchter et al. 2001; (18) Jakobsson et al. 2003; (19) Holland et al. 2002; (20) Price et al. 2003; (21) Berger et al. 2003; (22) Mirabal, Paerels & Halpern 2003; (23) Barth et al. 2003; (24) Covino et al. 2003; (25) Urata et al. 2003; (26) Møller et al. 2002; (27) Holland et al. 2003; (28) Greiner et al. 2003a; (29) Pandey et al. 2004; (30) Greiner et al. 2003c; (31) Sato et al. 2003; (32) Matheson et al. 2003;

TABLE 2  
*R*-BAND DATA OF FAST-FADING GRB AFTERGLOWS

GRB	<i>z</i>	$\alpha$	$t_j$ (days)	$F_{\nu,j}$ ( $\mu$ Jy)	$\beta_{\text{opt}} (t_{\text{day}})$	Reference
980326	$\sim 0.9$	$2.0 \pm 0.1$	$< 0.42$	$> 10.09^{+0.97}_{-0.89}$	$0.8 \pm 0.4(2.38)$	1
991208	0.7063	$2.30 \pm 0.07$	$< 2.1$	$> 100^{+9.6}_{-8.8}$	$1.05 \pm 0.09(3.8)^a$	2,3,2
000131	4.500	$2.25 \pm 0.19$	$< 3.513$	$> 1.5^{+0.036}_{-0.054}$	$\sim 0.70(3.5)$	4
000911	1.0585	$1.46 \pm 0.05$	$< 1.435$	$> 15.85^{+1.23}_{-1.14}$	$0.75 \pm 0.01(> 1.44)$	5,6
001007	...	$2.03 \pm 0.11$	$< 3.95$	$> 19.05^{+2.42}_{-2.15}$	$1.24 \pm 0.57(3.94)^a$	7

NOTE.—Col.(1) GRB name; col.(2) redshift; col.(3) temporal decay index ( $F_{\nu} \propto t^{-\alpha}$ ); col.(4) observed jet break time; col.(5) flux density at  $t_j$ ; col.(6) optical spectrum  $F_{\nu} \propto \nu^{-\beta_{\text{opt}}}$  at time  $t$  in days since the GRB trigger; and col.(7) references for the redshift and *R*-band afterglow. <sup>a</sup>The value is not de-reddening for the extinction of the host galaxy and the actual one may be flatter.

REFERENCES.— (1) Bloom et al. 1999; (2) Castro-Tirado et al. 2001; (3) Jensen et al. 1999; (4) Anderson et al. 2000; (5) Price et al. 2002; (6) Lazzati et al. 2001; (7) Castro Cerón et al. 2002;

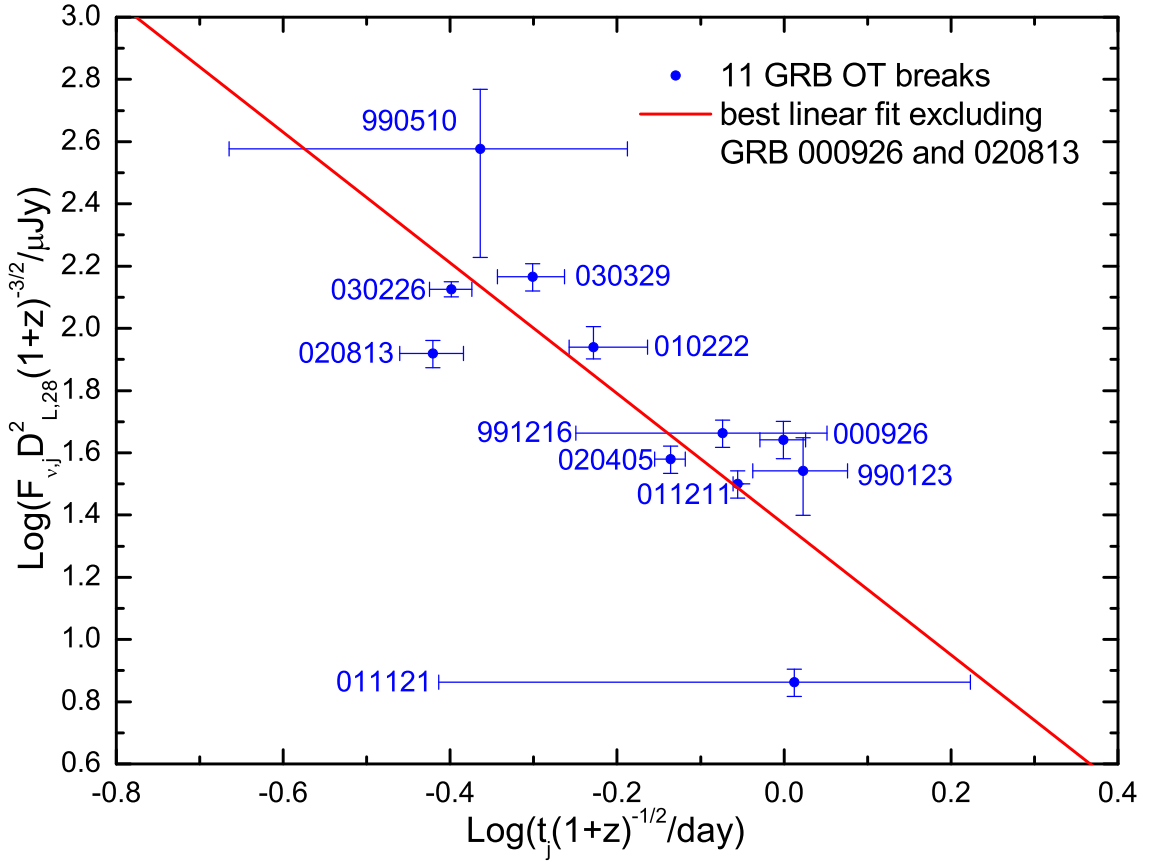


FIG. 1.— Plot of  $\mathcal{L}_J$  as a function of  $\tau_j$  for 11 well-observed GRB *R*-band jet break data with known redshifts listed in Table 1, excluding two peculiar GRB OTs (GRB 000310C and 021004). The solid line shows the best linear fit to these data for the slow-cooling jet break relation (i.e., eqs. [6] and [14]):  $a = 1.37 \pm 0.05$ ,  $b = 2.10 \pm 0.21$  ( $1\sigma$ ),  $\chi^2 = 9.97$  for  $9 - 2$  degrees of freedom, and the possibility  $Q(> \chi^2) = 0.19$ . The jet breaks of GRBs 000926 and 020813 are considered to be the fast-cooling ones by their spectra and therefore are not included in the linear fit.

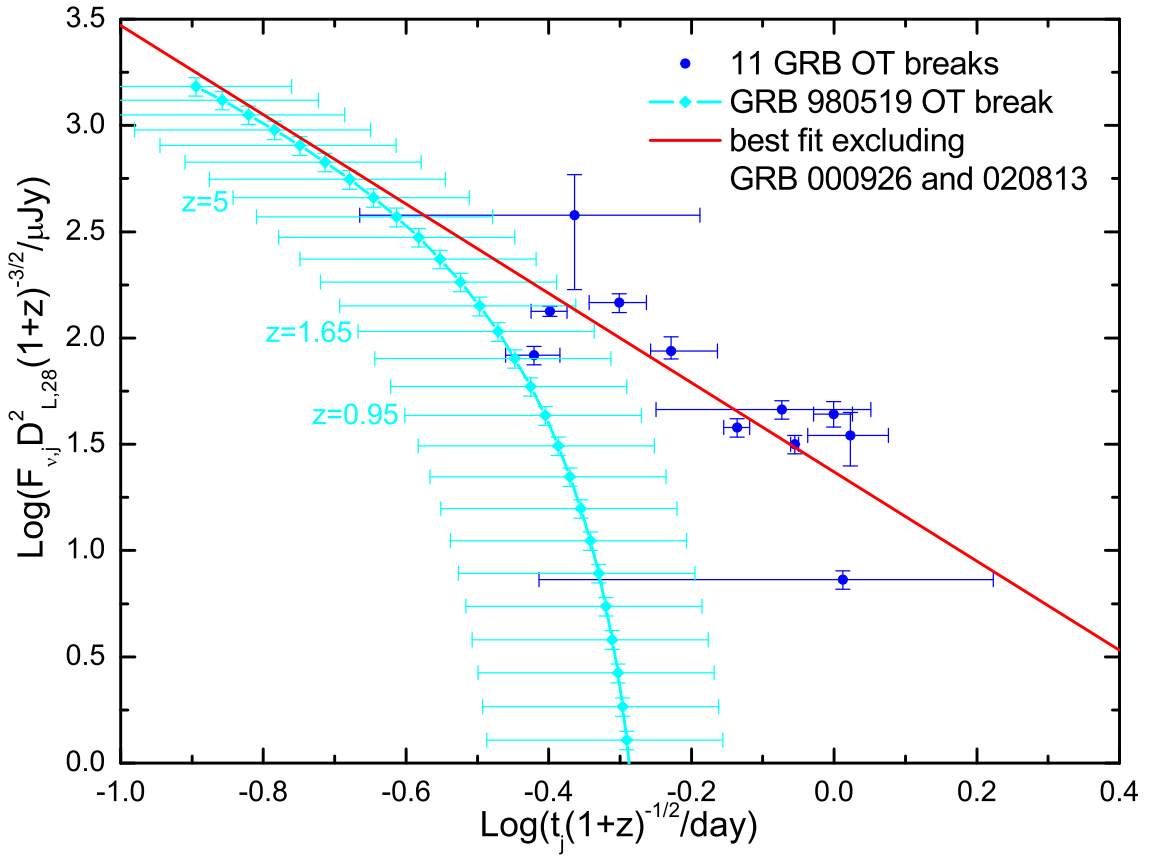


FIG. 2.— GRB 980519 *R*-band jet break data vary as redshift in the slow-cooling jet break plot. The solid line with  $a = 1.37 \pm 0.05$ ,  $b = 2.10 \pm 0.21$  is the best linear fit, similar to Fig. 1. GRB 980519 would lie at  $z \gtrsim 1.65$  if it obeys the same jet break relation.

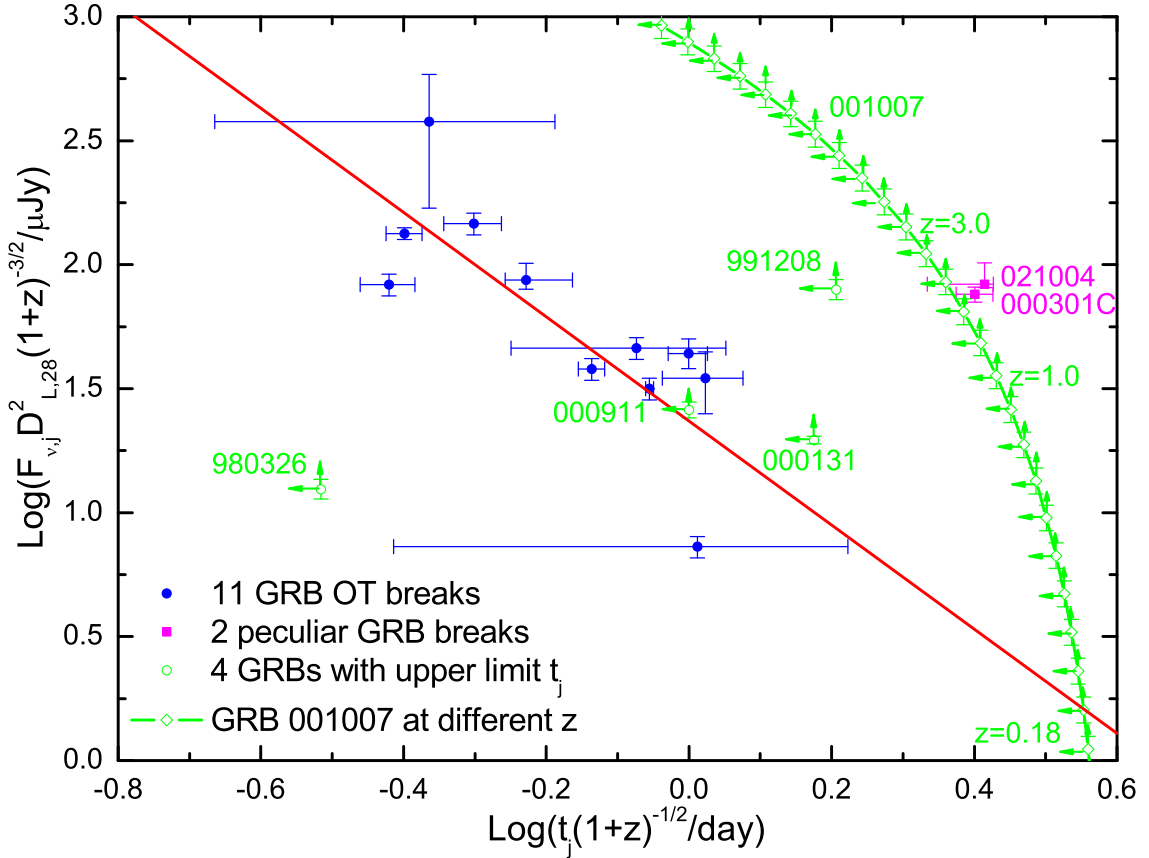


FIG. 3.— All  $R$ -band jet break data of 11 typical and two peculiar GRB OTs and upper limits of  $t_j$  of four fast-fading GRB OTs. The solid line with  $a = 1.37 \pm 0.05$  and  $b = 2.10 \pm 0.21$  is also shown for comparison. Two fast-fading OTs (GRBs 980326 and 991208) and the two peculiar GRB 000301C and 021004 OTs form distinctive classes (less energetic GRB 980326 and more energetic bursts for the three others) from the others. It can be estimated from the jet break relation that the redshift of the fast-fading GRB 001007 is  $z \sim 0.2$ .